# Chaos and noise in a truncated Toda potential

Salman Habib,[1,*] Henry E. Kandrup,[2,†] and M. Elaine Mahon[2,‡]
[1]*T-6, Theoretical Astrophysics and T-8, Elementary Particles and Field Theory, Los Alamos National Laboratory, Los Alamos, New Mexico 87545*
[2]*Department of Astronomy and Institute for Fundamental Theory, University of Florida, Gainesville, Florida 32611*
(Received 20 March 1995)

Results are reported from a numerical investigation of orbits in a truncated Toda potential that is perturbed by weak friction and noise. Aside from the perturbations displaying a simple scaling in the amplitude of the friction and noise, it is found that even very weak friction and noise can induce an extrinsic diffusion through cantori on a time scale that is much shorter than that associated with intrinsic diffusion in the unperturbed system. The results have applications in galactic dynamics and in the formation of a beam halo in charged particle beams.

PACS number(s): 05.45.+b, 05.40.+j

In the past several years, substantial interest has centered on the study of stochastic orbits in nonintegrable Hamiltonian systems. In particular, much work has focused on the phenomenon of intrinsic diffusion through cantori, e.g., using the "turnstile" model of MacKay, Meiss, and Percival [1], which leads to interesting scaling behavior [2], and, more recently [3], through the utilization of local Lyapunov exponents [4]. However, with a few notable exceptions (cf. [5]), little has been done to determine how the results derived from such analyses are changed if non-Hamiltonian perturbations are allowed. This is an issue of key importance given the connection between dynamical chaos and the foundations of classical statistical mechanics [6]. Furthermore, diffusion through cantori, catalyzed by weak noise (modeling, e.g., close encounters between stars) may be important for orbit dynamics studies of galaxies [7] and beam halo formation in intense, mismatched charged particle beams [8].

In modeling a physical system in terms of a few degrees of freedom Hamiltonian, one is usually implementing a reduced description, e.g., in terms of collective coordinates, that neglects (hopefully) weak couplings to an external environment and/or various (relatively) unimportant degrees of freedom. Such weak, and in principle unavoidable, corrections can often be viewed as a source of friction and noise, related via a fluctuation-dissipation theorem. Naively, one might expect that weak coupling to an environment should only have effects on very long time scales. While this expectation is true for quantities such as adiabatic invariants, it is not true in general. For chaotic systems such effects can in fact be important on time scales much shorter than the natural relaxation time scale. A potentially significant example is reported in this paper.

The system considered here is the sixth order truncation of the Toda [9,10] potential, which leads to the Hamiltonian

$$H=\tfrac{1}{2}(v_x^2+v_y^2)+\tfrac{1}{2}(x^2+y^2)+x^2y-\tfrac{1}{3}y^3+\tfrac{1}{2}x^4+x^2y^2+\tfrac{1}{2}y^4+x^4y+\tfrac{2}{3}x^2y^3-\tfrac{1}{3}y^5+\tfrac{1}{5}x^6+x^4y^2+\tfrac{1}{3}x^2y^4+\tfrac{11}{45}y^6\,, \tag{1}$$

where $\{x,v_x\}$ and $\{y,v_y\}$ represent conjugate pairs. This Hamiltonian is nonintegrable and its regular and stochastic regions have been characterized in Ref. [10]. The third order truncation of the Toda potential leads to the well-known Hénon-Heiles potential [11] used to model nonlinear dynamics in galaxies. The sixth order truncation was chosen to yield a bounded phase space: this is essential for the existence of an invariant measure.

The Hamiltonian evolution was perturbed by allowing for a constant friction $-\eta\mathbf{v}$ and $\delta$-correlated additive white noise $\mathbf{F}(t)$, related via a fluctuation-dissipation theorem with temperature $\Theta\sim E$. As described below, the principal conclusions have also been observed [7] in another nonintegrable potential.

For each initial condition, an unperturbed Hamiltonian trajectory was computed. Multiple Langevin simulations were then performed, using a numerical algorithm (cf. [12]) which generates a random $\mathbf{F}$ with the proper first and second moments. The total time for each integration was $t\leq 140$ (the dynamical or crossing time is of order unity and the time step $h=0.001$).

Viewed over long time scales, the unperturbed Hamiltonian trajectories divide naturally into only two classes, namely, regular orbits, with vanishing Lyapunov exponent, and stochastic orbits, with nonvanishing Lyapunov exponent. However, on shorter time scales, the stochastic orbits divide in turn into two relatively distinct types, namely, filling stochastic orbits, which travel unimpeded throughout the stochastic regions and confined, or sticky, stochastic orbits, which are trapped near islands of regularity by cantori [13], and only escape over much longer time scales. It is therefore meaningful to consider the effects of friction and noise separately on these three different orbit classes.

*Electronic address: habib@predator.lanl.gov
†Also at Department of Physics, University of Florida. Electronic address: kandrup@astro.ufl.edu
‡Electronic address: mahon@astro.ufl.edu

 

Experiments focused on the energy range $10 \leq E \leq 100$, with $10^{-12} \leq \eta \leq 10^{-3}$ and $0.1 \leq \Theta/E \leq 10.0$. Two different types of experiments were performed.

(1) For each of a large number of individual initial conditions, corresponding to both regular and stochastic orbits, $N=48$ different noisy realizations were effected. The orbits were compared to the unperturbed trajectories and analyzed statistically to extract the first and second moments of such quantities as the position, velocity, and energy, e.g.,

$$\langle |\delta E|^2 \rangle \equiv \delta E_{\rm rms}^2 \equiv \frac{1}{N} \sum_{i=1}^{N} (E_{\rm unp} - E_i)^2 \ . \tag{2}$$

(2) The near-invariant distribution associated with the Hamiltonian evolution was sampled to extract 400 initial conditions corresponding to stochastic orbits, and 100 noisy realizations were effected for each of these initial conditions. The outputs were then analyzed in two ways, (a) by comparing with the unperturbed trajectories to extract first and second moments which average over the ensemble of initial conditions, and (b) by binning the orbital data at fixed time intervals to study systematic changes in the form of the near-invariant distribution. The large number of initial conditions and realizations is needed to have acceptable statistics. The particular values of the friction coefficient were chosen so as to bracket the values of physical interest in galactic dynamics and beam transport [7,15].

Viewed in energy space, weak friction and noise serve to induce a classical diffusion process. Specifically, at least for early times, when $\delta E_{\rm rms}/E_{\rm unp} \ll 1$, $\delta E_{\rm rms}$ satisfies the simple scaling relation

$$\delta E_{\rm rms}^2 = A^2(E) E \eta \Theta t \ , \tag{3}$$

with $A(E)$ only weakly dependent on $E$. This scaling holds for all three classes of orbits, regular, sticky stochastic, and filling stochastic. It also holds for individual initial conditions as well as for ensembles of initial conditions. Viewed in energy space, one cannot distinguish between different orbit classes (which is as expected, since the energy is an invariant in the absence of friction and noise).

Viewed in configuration or velocity space, friction and noise have more complicated effects, the form of which depend on whether the orbit is regular, sticky stochastic, or filling stochastic. For regular orbits the second moments in position and velocity grow as a power law in $t$, albeit more rapidly than the analytically predicted relation $\delta x_{\rm rms}, \delta v_{v,\rm rms}, \ldots \propto t^{1/2}$ satisfied by the integrable cases of a harmonic oscillator or a free particle. By contrast, for stochastic orbits these rms quantities grow exponentially at a rate $\Lambda$ that is comparable in magnitude to the Lyapunov exponent $\chi$, which characterizes the average instability of the Hamiltonian orbit (see Fig. 1). This conclusion holds both for entire ensembles and for individual initial conditions. In the latter case, one also observes a direct correlation between the growth rate $\lambda_i$ for an individual initial condition and the local Lyapunov exponent $\chi_i$ for that initial condition. This behavior is consistent with the intuitive explanation that noise "blurs" a sharp classical trajectory and this "blur" is then

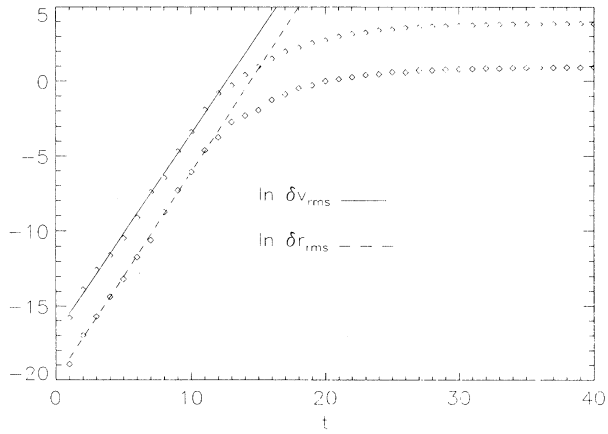


FIG. 1. The early time exponential growth of $\delta r_{\rm rms} \equiv (\delta x_{\rm rms}^2 + \delta y_{\rm rms}^2)^{1/2}$ (dashed curve) and the corresponding $\delta v_{\rm rms}$ (solid curve) for $E=30$ and $\eta = 10^{-9}$ is clearly apparent in this figure.

blown up by the chaotic dynamics on a time scale set by the maximal Lyapunov exponent. This correlation is particularly strong for the case of weak friction and noise. Moments for the confined stochastic orbits exhibit an intermediate behavior.

Despite these differences, the moments for all three classes of orbits exhibit a simple scaling in terms of $\Theta$ and $\eta$. Specifically, provided that the deviations have not become macroscopic (i.e., assuming $\delta x_{\rm rms}, \delta y_{\rm rms} \ll 1$), all three classes of orbits satisfy a scaling relation

$$\delta x_{\rm rms}, \delta y_{\rm rms}, \delta v_{x,\rm rms}, \delta v_{y,\rm rms} \propto \Theta^a \eta^b F(E,t) \ , \tag{4}$$

where $a=b=0.50 \pm 0.01$ for the range of values probed. This was confirmed both for multiple realizations of individual initial conditions and for ensembles of initial conditions corresponding to stochastic orbits. It follows that, even for stochastic orbits, one observes the same scaling in $\Theta$ and $\eta$ as for regular orbits in a harmonic oscillator potential, although the time dependence is extremely different.

Another common feature of all three orbit classes is that, at sufficiently early times, the time dependence is reasonably well fit by a power law, i.e.,

$$\delta x_{\rm rms}, \delta y_{\rm rms}, \delta v_{x,\rm rms}, \delta_{y,\rm rms} \propto \tilde{F}(E) \Theta^a \eta^b t^c \ . \tag{5}$$

The interval over which such a fit is appropriate depends on the orbit class: filling stochastic orbits rapidly begin to show an exponential divergence, confined stochastic orbits only somewhat later, and regular orbits continue to manifest an approximate power law growth. The best fit value of $c$ depends on the sampling interval: Fitting for relatively short times yields a value $c \approx 1.10-1.25$. Fitting regular orbits over longer times yields $c \approx 1.20-1.50$.

To investigate the generality of these scaling relations, simulations were also performed for the dihedral $D4$ potential of Ref. [14], with a choice of parameter values which leads to a large amount of stochasticity. Specifically, the Hamiltonian was taken to be of the form

$$H = \tfrac{1}{2}(v_x^2 + v_y^2) - (M/2)(x^2+y^2) - (a/4)(x^2+y^2)^2 - (b/2)x^2 y^2 \ , \tag{6}$$

with $M=2$, $a=-1$, and $b=\frac{1}{2}$.

Analysis of these simulations shows once again a scaling of the form given by (4) and (5), with the same values $a=b=0.50\pm0.01$. The best fit $c$ for Eq. (5) shows more variability from run to run, so that a detailed comparison is difficult to effect. However, the data are consistent with the conclusion that $c$ is the same for both models. When viewed in energy space, friction and noise again induce a simple diffusion process of the form (3) for the $D4$ potential.

Generic ensembles of initial conditions corresponding to filling stochastic orbits, when evolved with the truncated Toda Hamiltonian (1), exhibit a coarse-grained exponential evolution towards an approximately invariant distribution [3]. For high energies $E \geq 50$, where the regular regions are very small, this distribution appears to correspond to a true invariant measure. However, for lower energies, where the relative measure of the regular regions is larger, this distribution slowly changes in form over longer time scales. As a result of intrinsic diffusion, the orbits can pass through the cantori to occupy phase space regions near the regular islands from which they were excluded at earlier times.

At a coarse-grained level, an ensemble of orbits can be characterized numerically by binned, projected distributions, such as $f(x,y,t;\Delta t)$ or $f(y,v_y,t;\Delta t)$, constructed by averaging the binned orbital data over some time interval $\Delta t$ [3]. In order to compare two different distributions $f_1$ and $f_2$, one requires a notion of distance. This was provided through the introduction of a coarse-grained $L^1$ norm: For two identically normalized distributions, $f_1(x,y)$ and $f_2(x,y)$, binned in an $n\times n$ grid of cells of size $\{\Delta x,\Delta y\}$,

$$Df_{1,2}(x,y)=\sum_{i=1}^{n}\sum_{j=1}^{n}|f_1(x,y)-f_2(x,y)|\Big/\sum_{i=1}^{n}f_1(x,y)\ . \tag{7}$$

It is with respect to this measure of distance that the Hamiltonian flow evidences an evolution towards a near-invariant measure.

However, if this near-invariant measure were evolved into the future, allowing for even weak friction and noise, one can observe systematic changes on time scales much shorter than the intrinsic diffusion time scale. The friction and noise can induce a significant extrinsic diffusion which allows filling stochastic orbits to become confined, thereby populating regions of the phase space near regular islands which were avoided by the deterministic near-invariant measure.

The Hamiltonian evolution conserves energy, restricting orbits to a constant energy hypersurface. When friction and noise are included, the energy is no longer conserved. However, it is approximately conserved over sufficiently short time scales, so that one can still speak of an "almost constant energy hypersurface." It is therefore meaningful to quantify the degree to which friction and noise alter the form of the near-invariant distribution on a near-constant energy hypersurface.

For the Toda potential, the observed changes are larger for lower energies, where the regular regions comprise a bigger fraction of the available phase space. The case of $E=30$, where cantori are very important, is particularly illuminating. For $\eta=10^{-6}$, there is clear evidence that the noisy ensemble is evolving towards a new distribution which, over times scales $t\sim100$, is approximately time independent. For $\eta=10^{-9}$, there is again a nontrivial time evolution, but the changes occur too slowly to see clear evidence of an approach towards a new

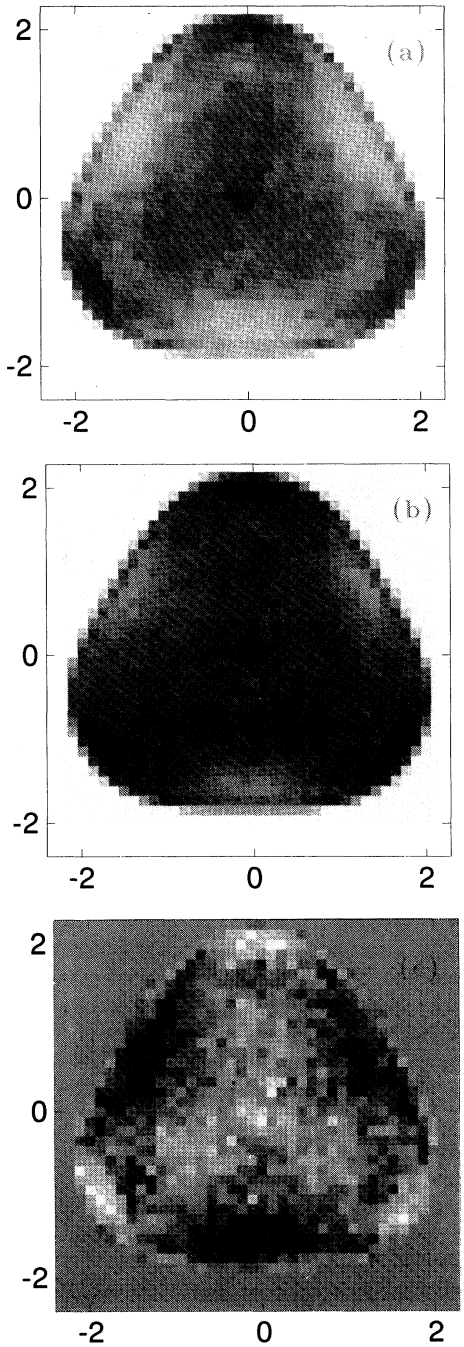


FIG. 2. (a) A gray scale plot of the deterministic near-invariant $f_0(x,y)$ for $E=30$, generated from a $40\times40$ binning. Darker shades represent higher densities. (b) The corresponding gray scale plot for the near-invariant $f_\eta(x,y)$ for $E=30$ and $\eta=10^{-6}$. (c) The difference $f_0(x,y)-f_\eta(x,y)$.

time-independent form. For $\eta=10^{-4}$, changes in the energy are too large to speak of an approximately constant energy hypersurface. However, the data are still consistent with an evolution towards a modified distribution in which cantori around the regular regions have been breached.

This behavior is illustrated for $E=30$ in Fig. 2. The first panel shows the form of the near-invariant distribution $f_0(x,y)$ associated with the deterministic evolution. The second panel shows the form of the noisy near-invariant distribution $f_\eta(x,y)$ for $\eta=10^{-6}$. The final panel exhibits the difference $f_0(x,y)-f_\eta(x,y)$. The deterministic distribution $f_0(x,y)$ has four sharp relative minima which have become blurred somewhat in the noisy $f_\eta(x,y)$ by the diffusion of orbits into lower density regions. Both here and for other energies, the evolution from $f_0$ to $f_\eta$ is well fit by an exponential, with a rate $\Lambda$ that scales roughly as $\ln\eta$. For a $10\times10$ binning, the best fit values for the slope are, for $\eta=10^{-9}$, $\Lambda=-0.0143$; for $\eta=10^{-6}$, $\Lambda=-0.0339$; and for $\eta=10^{-4}$, $\Lambda=-0.0460$.

The fact that orbits can pass through cantori, going either in or out, implies the possibility of changes in orbit class between filling and confined stochastic orbits. It is difficult to construct a simple numerical algorithm to decide when an orbit has changed class. However, visual inspection of a large number of orbits ($\sim10^4$) leads to qualitative conclusions that are easily summarized. At high energies, $E\geq50$, changes in orbit class are infrequent since the size of the phase space region restricted by cantori is relatively small. However, for lower energies, these regions become larger and changes in orbit class more common.

This can be quantified by determining the minimum amplitude of friction and noise required to induce one or more changes in orbit class for a significant fraction of the orbits within time $t=100$. Consider, e.g., the case $E=20$ and $\Theta\sim E$. For $\eta\ll10^{-9}$, the friction and noise are too weak to cause a significant number of orbits to change class. However, for $\eta\sim10^{-9}$, friction and noise begin to become more important, and, already for $\eta=10^{-6}$, as many as 50% of the noisy realizations for any initial condition can result in a change between filling and confined stochastic. Such changes are not accompanied by changes between regular and stochastic orbits, which, deterministically, are separated by KAM tori, rather than cantori. Only for $\eta\geq10^{-3}$ are many such changes observed.

What these simulations imply is that even very weak friction and noise, with characteristic time scale $t_R\geq10^6$ characteristic crossing times $t_{\rm cr}$ can have significant effects within a time as short as $\sim10^2t_{\rm cr}$. This has important implications for problems in galactic dynamics and beam halo formation in charged particle beams.

In galactic dynamics attention focuses on the construction of models of galaxies which involve ensembles of orbits evolving in a self-consistently determined potential, ignoring all non-Hamiltonian irregularities. The calculations reported here suggest that such self-consistent models could differ substantially from the types of objects which might arise in nature if one were to allow for these irregularities. In particular, confined stochastic orbits have been used to help support structures such as bars in phase space regions such as corotation where, owing to resonance overlap, few, if any, regular orbits exist. However, if noise facilitates enhanced diffusion through cantori, it could serve to destabilize certain structures and/or lead to the formation of other new structures in a time scale well within the age of the Universe.

The newly developed "core-halo" model describes the beam halo in mismatched charged particle beams [8]. In this model, the transverse motion of the halo particles is chaotic, and particles initially in the beam core can leak out through a broken separatrix and be carried to large amplitudes. This is a serious design issue for high intensity linacs planned for future accelerator-driven technologies. Particle-particle scattering and fluctuations in the external electromagnetic fields can provide a mechanism for halo formation; the results of this paper indicate that the halo may be formed much more rapidly than the simple diffusion time estimate. This possibility is now under investigation [15].

The authors acknowledge useful discussions with John Klauder, Ed Ott, Jim Peebles, Robert Ryne, and Tom Wangler. S. H. was supported in part by the DOE and by AFOSR. H. E. K. was supported by NSF Grant No. PHY92-03333. M. E. M. was supported by the University of Florida. Computer time was made available through the Research Computing Initiative at the Northeast Regional Data Center (Florida) by the IBM Corp. and by the Advanced Computing Laboratory at Los Alamos National Laboratory.

[1] R. S. MacKay *et al.*, Phys. Rev. Lett. **52**, 697 (1984).
[2] Y.-T. Lau, J. M. Finn, and E. Ott, Phys. Rev. Lett. **66**, 978 (1991); J. D. Meiss and E. Ott, *ibid.* **55**, 271 (1985).
[3] H. E. Kandrup and M. E. Mahon, Phys. Rev. E **49**, 3735 (1994); Astron. Astrophys. **290**, 762 (1994).
[4] P. Grassberger *et al.*, J. Stat. Phys. **51**, 135 (1988); M. A. Sepúlveda *et al.*, Phys. Rev. Lett. **63**, 1226 (1989).
[5] M. A. Lieberman and A. J. Lichtenberg, Phys. Rev. A **5**, 1852 (1972).
[6] See, e.g., M. Toda, R. Kubo, and N. Hashitsume, *Statistical Physics. II* (Springer-Verlag, Berlin, 1991).
[7] S. Habib, H. E. Kandrup, and M. E. Mahon (unpublished).
[8] See, e.g., T. P. Wangler, Los Alamos National Laboratory Report No. LAUR-94-1135, 1994 (unpublished); J.-M. Lagniel, Nucl. Instrum. Methods Phys. Res. Sec. A **345**, 46 (1994); R. L. Gluckstern, Phys. Rev. Lett. **73**, 1247 (1994); S. Habib and R. D. Ryne, *ibid.* **74**, 70 (1995).
[9] M. Toda, J. Phys. Soc. Jpn. **22**, 431 (1967).
[10] G. Contopoulos and C. Polymilis, Physica D **24**, 328 (1987).
[11] M. Hénon and C. Heiles, Astrophys. J. **69**, 73 (1964).
[12] A. Greiner *et al.*, J. Stat. Phys. **51**, 95 (1988).
[13] J. N. Mather, Topology **21**, 45 (1982).
[14] D. Armbruster *et al.*, Phys. Lett. A **140**, 419 (1989).
[15] S. Habib, R. D. Ryne, and T. P. Wangler (unpublished).

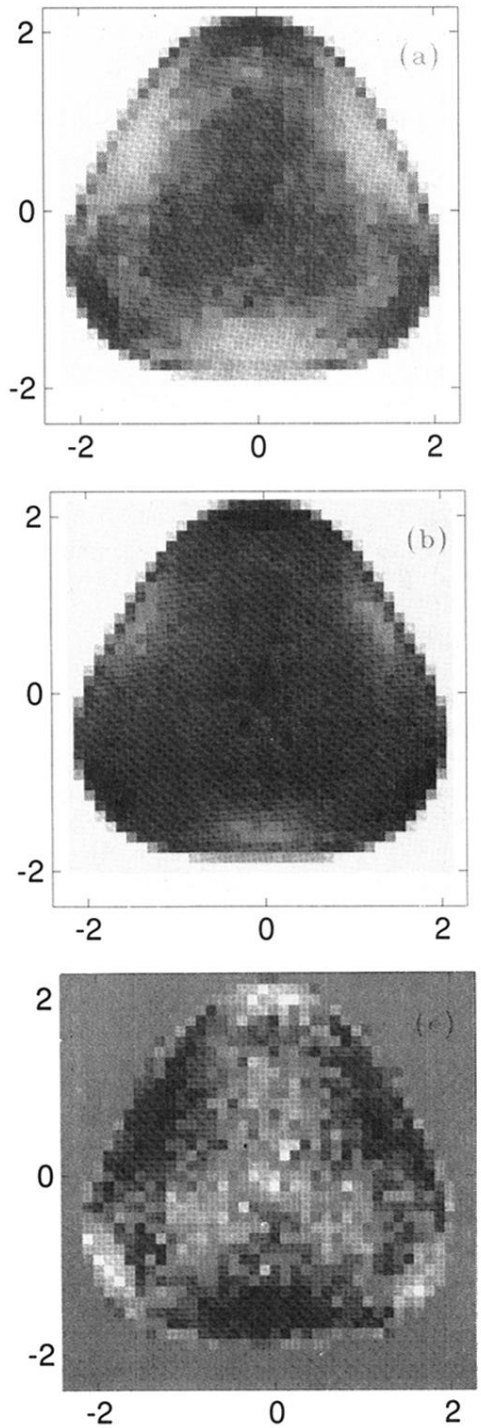


FIG. 2. (a) A gray scale plot of the deterministic near-invariant $f_0(x,y)$ for $E=30$, generated from a $40\times40$ binning. Darker shades represent higher densities. (b) The corresponding gray scale plot for the near-invariant $f_\eta(x,y)$ for $E=30$ and $\eta=10^{-6}$. (c) The difference $f_0(x,y)-f_\eta(x,y)$.